

AD-A193 147

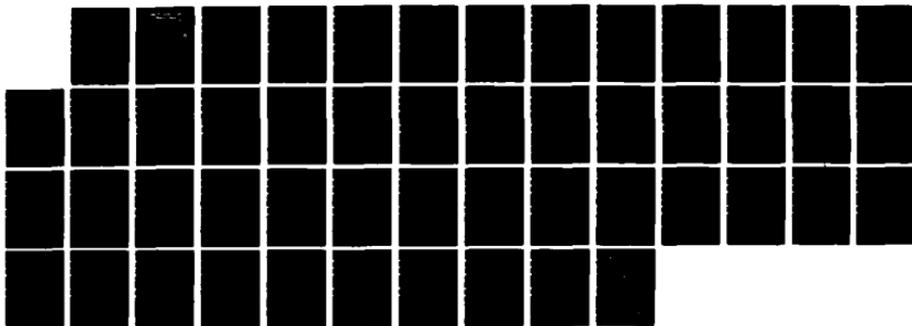
THE INFLUENCE OF IONIZATION WITHIN A PLASMA OPENING  
SWITCH(U) NAVAL POSTGRADUATE SCHOOL MONTEREY CA  
W G EVANS DEC 87

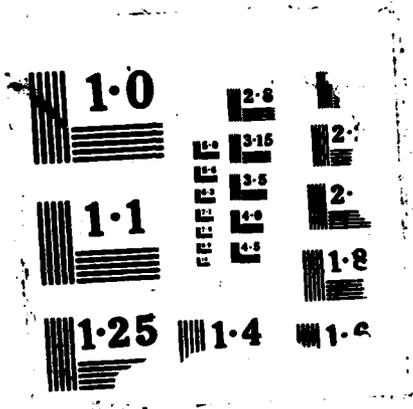
1/1

UNCLASSIFIED

F/G 9/1

NL





2

# NAVAL POSTGRADUATE SCHOOL Monterey, California

DTIC FILE COPY

AD-A193 147



DTIC  
ELECTE  
MAY 26 1988  
S D

## THESIS

THE INFLUENCE OF IONIZATION WITHIN A  
PLASMA OPENING SWITCH

by

Wenzel G. Evans, Jr.

December 1987

Thesis Advisor: Fred R. Schwirzke

Approved for public release; distribution is unlimited

003

UNCLASSIFIED

SECURITY CLASSIFICATION OF THIS PAGE

## REPORT DOCUMENTATION PAGE

1a REPORT SECURITY CLASSIFICATION <b>UNCLASSIFIED</b>		1b RESTRICTIVE MARKINGS	
2a SECURITY CLASSIFICATION AUTHORITY		3 DISTRIBUTION/AVAILABILITY OF REPORT Approved for public release; distribution is unlimited.	
2b DECLASSIFICATION/DOWNGRADING SCHEDULE		5 MONITORING ORGANIZATION REPORT NUMBER(S)	
4 PERFORMING ORGANIZATION REPORT NUMBER(S)		7a NAME OF MONITORING ORGANIZATION Naval Postgraduate School	
6a NAME OF PERFORMING ORGANIZATION Naval Postgraduate School	6b OFFICE SYMBOL (if applicable)	7b ADDRESS (City, State, and ZIP Code) Monterey, California 93943-5000	
6c ADDRESS (City, State, and ZIP Code) Monterey, California 93943-5000		9 PROCUREMENT INSTRUMENT IDENTIFICATION NUMBER	
8a NAME OF FUNDING/SPONSORING ORGANIZATION	8b OFFICE SYMBOL (if applicable)	10 SOURCE OF FUNDING NUMBERS	
8c ADDRESS (City, State, and ZIP Code)		PROGRAM ELEMENT NO	PROJECT NO
		TASK NO	WORK UNIT ACCESSION NO
11 TITLE (include Security Classification) <b>THE INFLUENCE OF IONIZATION WITHIN A PLASMA OPENING SWITCH</b>			
12 PERSONAL AUTHOR(S) Evans, Wenzel G.			
13a TYPE OF REPORT Master's Thesis	13b TIME COVERED FROM TO	14 DATE OF REPORT (Year, Month Day) 1987 December	15 PAGE COUNT 49
16 SUPPLEMENTARY NOTATION			
17 COSATI CODES		18 SUBJECT TERMS (Continue on reverse if necessary and identify by block number)	
FIELD	GROUP	Plasma Opening Switch, Plasma Sheath Model	
	SUB-GROUP		
19 ABSTRACT (Continue on reverse if necessary and identify by block number) An alternate description of the Plasma Opening Switch (POS) is presented. In addition, a preliminary study was conducted into the ionization of desorbed carbon particles from the cathode surface in the switch region. The formation of a locally dense plasma layer surrounding the cathode is shown to influence the electric field and the Debye screening distance. This effect influences the emission of electrons from the cathode as well as providing a mechanism for opening the switch. <i>Howards</i>			
20 DISTRIBUTION/AVAILABILITY OF ABSTRACT <input checked="" type="checkbox"/> UNCLASSIFIED/UNLIMITED <input type="checkbox"/> SAME AS RPT <input type="checkbox"/> DTIC USERS		21 ABSTRACT SECURITY CLASSIFICATION <b>UNCLASSIFIED</b>	
22a NAME OF RESPONSIBLE INDIVIDUAL Fred R. Schwirzke		22b TELEPHONE (include Area Code) 408 646-2683	22c OFFICE SYMBOL Code 61Sw

DD FORM 1473, 84 MAR

83 APR edition may be used until exhausted  
All other editions are obsolete

SECURITY CLASSIFICATION OF THIS PAGE

UNCLASSIFIED

Approved for public release; distribution is unlimited

The Influence of Ionization Within a Plasma Opening Switch

by

Wenzel G. Evans, Jr.  
Captain, United States Army  
B.S., United States Military Academy, 1978

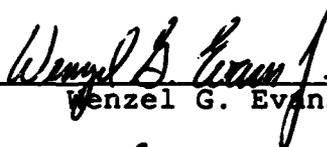
Submitted in partial fulfillment of the  
requirements for the degree

MASTER OF SCIENCE IN PHYSICS

from the

NAVAL POSTGRADUATE SCHOOL  
December 1987

Author:



Wenzel G. Evans, Jr.

Approved by:



F. Schwirzke, Thesis Advisor



K. E. Woehler, Second Reader



K. E. Woehler, Chairman, Department of Physics



G. E. Schacher, Dean of Science and Engineering

ABSTRACT

An alternate description of the Plasma Opening Switch (POS) is presented. In addition, a preliminary study was conducted into the ionization of desorbed carbon particles from the cathode surface in the switch region. The formation of a locally dense plasma layer surrounding the cathode is shown to influence the electric field and the Debye screening distance. This effect influences the emission of electrons from the cathode as well as providing a mechanism for opening the switch.



Accession For	
NWS CR4&I	<input checked="" type="checkbox"/>
DTIC TAB	<input type="checkbox"/>
Unannounced	<input type="checkbox"/>
Justification	
By	
Distribution	
Availability Codes	
Dist	Avail and/or Special
A-1	

## TABLE OF CONTENTS

I.	INTRODUCTION-----	7
	A. BACKGROUND-----	7
	B. THEORETICAL MODEL OF THE PEOS-----	8
	C. PLASMA SHEATH MODEL-----	9
	D. PURPOSE OF THE RESEARCH-----	10
II.	PLASMA SHEATH MODEL-----	11
	A. OVERVIEW-----	11
	1. Purpose of the Model-----	11
	2. Opening Switch Description-----	11
	B. PLASMA SHEATH DESCRIPTION-----	12
	1. Assumptions-----	12
	2. Desorption-----	13
	3. Initial Field Emission-----	14
	4. Ionization-----	15
	5. Ion Removal-----	16
	6. Magnetic Insulation-----	16
III.	IONIZATION OF NEUTRAL PARTICLES-----	18
	A. DESORBED NEUTRALS-----	18
	B. NEUTRAL DENSITY PROFILE-----	19
	C. ELECTRON FLUX-----	21
	D. DENSITY OF IONIZED PARTICLES-----	22
	E. DENSITY RATIO AND PRESSURE GRADIENT-----	24
IV.	RESULTS-----	26
	A. IONIZATION RATIO-----	26
	1. Density profile-----	27
	2. Desorbed layers-----	27
	3. Electron energy variations-----	30
	4. Delay time-----	32
	5. Plasma gun density-----	32

B.	PLASMA DENSITY GRADIENT EFFECT-----	32
V.	CONCLUSIONS-----	38
	LIST OF REFERENCES-----	40
	APPENDIX A: NEUTRAL DENSITY PROFILE-----	42
	APPENDIX B: PROGRAM LISTING-----	44
	INITIAL DISTRIBUTION LIST-----	48

#### ACKNOWLEDGEMENTS

I would like to thank Professor Schwirzke for his efforts in guiding me through this research. I also want to thank Professor Woehler for his patience and assistance during my schooling.

I especially want to thank my wife for her patience and assistance during this project. Her support and understanding was greatly appreciated.

## I. INTRODUCTION

### A. BACKGROUND

Inductive energy storage systems are capable of storing energy at densities up to 100 times that of capacitive systems [Ref. 1]. However, inductive storage systems are dependent on their opening switch characteristics. Switches range in type from mechanical (slow) to exploding fuses (faster) to plasmas (fastest).

The voltage output provided by an inductor is given by  $V = -L di/dt$ , where  $L$  [H] is the inductance and  $di/dt$  [A/s] is the changing current. As the switch determines the  $di/dt$  term, it is clear that faster switch performance can provide larger voltage/power output with smaller input current sources.

Currently, plasma switches are being incorporated into vacuum inductors to provide the fast switching necessary for pulsed-power applications. Of particular interest is the Plasma Opening Switch (POS). The POS has been used in experiments with the Gamble I [Ref. 1] and the Gamble II [Ref. 2] accelerators at the the Naval Research Laboratory (NRL) as well as with the Pollux and Kalif pulsed-power generators [Ref. 3] at the Kernforschungszentrum in Karlsruhe, West Germany. The results of these experiments have demonstrated that the POS was capable of conducting very

large currents before opening in less than 10 ns. Meger [Ref. 1] reported voltage and power multiplication of 2 and 4 times that of experiments without the switch while Ottinger reported similar results from experiments using the Gamble II accelerator [Ref. 2]. The POS was renamed the Plasma Erosion Opening Switch (PEOS) when Ottinger presented his theoretical model of the switch [Ref. 4].

The Naval Research Laboratory has been actively using the PEOS to provide pulse compression for their experiments involving a plasma radiation source (PRS). These experiments, sponsored by the Defense Nuclear Agency (DNA), were undertaken to develop a source which simulates the radiation produced by nuclear explosions. The results of these experiments have demonstrated that the performance of the PRS was directly affected by the use of the PEOS. The PEOS significantly reduced the prepulse and compressed the power pulse rise-time. This effectively inhibited the growth of instabilities in the plasma radiation source and produced a more efficient yield. [Ref. 2]

#### B. THEORETICAL MODEL OF THE PEOS

A theoretical model of the PEOS has been developed by Ottinger [Ref. 4] consisting of four phases: conduction phase, erosion phase, enhanced erosion phase and magnetic insulation phase. A complete description is available in Reference 4.

During the May 1986 DNA Pulsed-Power Review Meeting in Las Vegas, Nevada, the Maxwell Laboratory presentation reported the results of their latest PEOS experiments on the BlackJack 5 generator. The results demonstrated PEOS switching of currents up to 2 mega ampere with prepulse suppression. However, the report also indicated that the switch opened too slowly for pulsed power applications and that the magnetic insulation of the cathode surface was incomplete. The conclusions stated that critical aspects of the switch parameters and the physical mechanisms of the PEOS model were not well understood. [Ref. 5]

Schwirzke has asserted that the ion diode modeling of the PEOS is not applicable and the physics describing the plasma switch are incomplete. He has proposed an alternate description of the physical processes of the switch based on reduced field emission of electrons from the cathode surface.

#### C. PLASMA SHEATH MODEL

The proposed model is based on Schwirzke's earlier work [Ref. 6] and the recent work of Halbritter [Ref. 7]. These experiments demonstrated:

- \* Plasmas in contact with metals induced significant desorption of gases and other impurities from the surface.
- \* Electron field emission at contaminated surfaces is achieved with reduced electric fields.

These observed results led Schwirzke to postulate an alternate description to the PEOS model.

Schwirzke has asserted that Ottinger's PEOS model does not fully describe the physics of the switch. Schwirzke's major points of disagreement are:

- \* The electron current is field emitted rather than space-charge-limited.
- \* The sheath that forms between the bulk plasma and the cathode surface adjusts to the applied voltage at the cathode rather than being fixed.
- \* There is no physical mechanism which causes the PEOS gap to increase.

#### D. PURPOSE OF THE RESEARCH

The purpose of this research is to qualitatively describe Schwirzke's opening switch model and perform some preliminary testing to explore the influence of the neutral carbon ionization on the performance of the switch. Other aspects of the model will be treated qualitatively. It is hoped that this research will serve as a basis for the continued development of this model and that important insight into the switching behavior of the plasma can be achieved.

## II. PLASMA SHEATH MODEL

### A. OVERVIEW

#### 1. Purpose of the Model

The proposed plasma sheath model is an alternate description of the switch model known as the Plasma Erosion Opening Switch which has been developed by Ottinger [Ref. 4]. The plasma sheath model is based on the reduced field emission of electrons from a contaminated cathode surface. This model attempts to simplify and gain insight to the understanding of the physical behavior of a highly non-uniform plasma within a confined switch region.

#### 2. Opening Switch Description

The basic configuration of experiments using the plasma opening switch (POS) is shown in Figure 1. It consists of a generator section, vacuum coaxial inductor section, switch section and load section. Plasma is injected from plasma guns located off-axis toward the cathode. After a delay period, the generator is fired and current begins flowing from the outer anode to the inner cathode through the plasma switch region. The switch region conducts the current flow for some period of time before opening quickly and providing a high voltage pulse to the load section. It has been shown that the performance of the opening switch is highly dependent on the plasma density, the delay time for

firing the generator and the physical dimensions of the switch region. [Ref. 8]

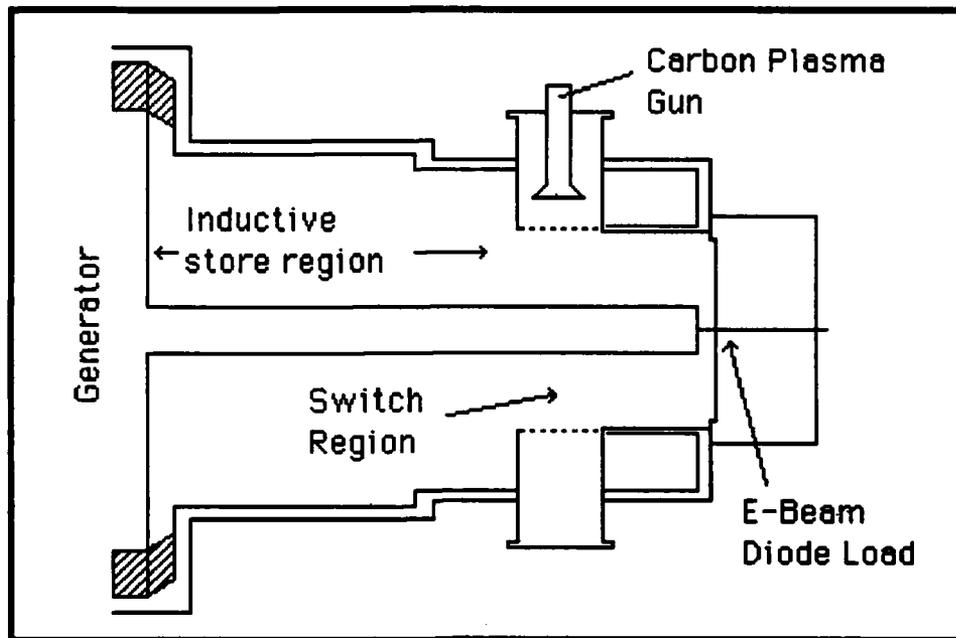


Figure 1. Experimental Setup

## B. PLASMA SHEATH DESCRIPTION

### 1. Assumptions

The major assumptions which apply to this model are:

- \* The anode-cathode potential difference is applied over the sheath region. The effective resistance of the bulk plasma is very small and it is determined by the Spitzer resistivity and the switch region dimensions. The potential difference required to drive the current through the bulk plasma is minimal and can be neglected compared to the total anode-cathode potential difference.
- \* The stainless steel cathode has several monolayers of contaminants on the surface. The main source of the contaminants is from the carbon plasma guns. After each firing of the plasma guns, a certain amount of residue settles on the surface of the cathode. For the purposes of this research, only the carbon neutrals will be considered.

- \* The streaming gun plasma induces desorption of the cathode surface contaminants. The desorbed contaminants expand, forming a dense layer or cloud of neutral particles. These particles are ionized by the emitted electrons from the cathode surface.
- \* The initial current flow in the switch region is uniform and in the radial direction. The field emitted electrons, normally emitted at very small sites such as whiskers or dirt spots, are considered to be distributed over the entire cathode surface in the switching region. In addition, the ion flow is considered to be uniform with a constant drift velocity toward the cathode.
- \* The switch dimensions and the density of the bulk plasma remain constant throughout the duration of the switching period. The density of the bulk plasma is confined without losses through any boundaries with the exception of the ion current at the cathode surface. However, this loss is small and can be neglected so that the plasma density is essentially constant.
- \* The sheath region does not break down due to the voltages across the gap. In addition, the plasma temperature assumes the energy of the cathode. As the cathode energy increases, the sheath distance increases by pushing the electrons further away. This imparts energy to these electrons which in turn is applied to the bulk plasma.
- \* The cathode is cold so that thermal emission of electrons is not significant and can therefore be neglected.

## 2. Desorption

As the injected plasma comes into contact with the cathode, the neutral contaminant layers are disrupted and these atoms are desorbed from the surface. These neutrals expand slowly (approximately 330 m/s) and form a locally dense layer of atoms to be ionized. The expansion of the neutral particles is considered only during the time period that the plasma is in contact with the cathode surface prior to the firing of the generator. This is due to the slow

expansion velocity and very short time frame for current conduction. Therefore, the number of neutral particles desorbed and the distance traveled from the cathode surface is considered constant throughout the switching phase.

### 3. Initial Field Emission

The initial emission of electrons from the cathode surface is produced by localized spots with high electric field strengths. The electric field,  $E$  (V/m) is enhanced by a factor  $\beta$  such that the enhanced field is given by  $F = \beta E$ . The enhancement factor range is  $10 \leq \beta \leq 1000$ .

Halbritter's work [Ref. 7] demonstrated that the electron field emission current from contaminated surfaces was observed at electric field strengths on the order of  $F = 10^7$  V/m. The contributing factors to field enhancement are dust particles, whiskers and other contaminants.

The electric field is defined as  $E = -\nabla\phi$ , where  $\phi$  [V] is the potential field. For the case of cylindrical coordinates and a potential field which only varies in the radial direction, then  $E = -d\phi/dr$ . Furthermore, if it is assumed that  $d\phi/dr$  is constant within a given region, then  $E$  can be approximated by the potential difference over that region.

The plasma sheath model assumes that the anode-cathode potential difference occurs within a sheath region given by

$$\lambda_D = \left[ \frac{\epsilon_0 e \phi_c}{n e^2} \right]^{1/2} \quad (1)$$

where  $\epsilon_0$  [F/m] is the permittivity of free space,  $e$  [C] is the elementary charge,  $\phi_c$  [V] is the cathode potential and  $n$  [ $m^{-3}$ ] is the electron density of the plasma. This is the Debye screening distance for a negatively biased cathode. As stated earlier,  $E \sim \phi/\lambda_D$ , so that  $E$  varies with the plasma density and cathode potential as

$$E = \left[ \frac{n e \phi_c}{\epsilon_0} \right]^{1/2} \quad (2)$$

#### 4. Ionization

The ionization rate of the neutral particles is dependent on the neutral density, ionization cross section and the number of incident electrons. This research considers only the neutral carbon atoms which are ejected from the surface for calculations of the ionization cross section.

As the neutrals become ionized, a locally more dense plasma forms near the cathode surface which influences the electric field and the sheath width. From Equation 2, it is clear that for a constant potential, the electric field varies with the density. For increasing density, the

electric field strength increases and additional field emission from the cathode is possible.

#### 5. Ion Removal

The ionization of the neutral particles produces a locally more dense plasma near the cathode surface. The ionized particles in the sheath, under the influence of an enhanced electric field, are accelerated toward the cathode surface. The time required for these ions to reach the surface is determined by the accelerating field and the distance traveled. As the carbon ions are removed from the sheath region, they contribute to the total ion current flow due to the higher density. In addition, the reduction in the local charge density causes the sheath width to increase and the electric field to decrease. As the magnetic field strength increases, the electrons begin to drift toward the load side of the switch before crossing the gap and entering the bulk plasma.

#### 6. Magnetic Insulation

Magnetic insulation occurs when the magnetic field near the cathode is sufficiently large to cause the electron Larmor radius to be smaller than the sheath width. As the magnetic field experienced by the emitted electrons increases, the electrons experience the  $E \times B$  ( $E$  is assumed to be radial and  $B$  is in the  $\theta$  direction) drift which causes the electrons to drift parallel ( $z$  direction) to the cathode surface for the length of the switch. The current is

switched to the load and the effective switch resistance increases. The switch is considered open when the Larmor radius becomes less than the sheath width.

### III. IONIZATION OF NEUTRAL PARTICLES

There are four critical areas of interest in the plasma sheath model which need to be addressed. These are:

- \* The ionization of neutral particles which are desorbed from the cathode surface.
- \* Electric field strength and sheath width response due to the increased ionization of neutral particles.
- \* Ion removal occurring at the cathode surface.
- \* Magnetic insulation which causes the switch to open.

This section is devoted to the calculations necessary to determine the number and density profiles of the desorbed carbon atoms, the number and density profile of the newly formed plasma and the electric field produced by the pressure force associated with a density gradient. The computations used are based on fundamental plasma physics relationships. No effort has been made to apply statistical methods to this problem.

#### A. DESORBED NEUTRALS

The cathode used in the experiments at the Naval Research Laboratory and at the Kernforschungszentrum in Karlsruhe is made of stainless steel. Most stainless steels consist of a small percentage of nickel and chromium (usually below 20%) mixed in with the base metal of iron. At temperatures below 912 degrees Celsius, the crystal lattice structure of iron is

body centered cubic (BCC) with a lattice parameter of  $2.866 \times 10^{-10}$  meters. The contaminants, which are situated on the surface, will occupy the interstitial sites. Therefore, the BCC configuration and lattice parameter of iron will be used for the calculation of the number of carbon particles desorbed from the cathode surface. [Ref. 8]

The volume of a layer on the cathode surface within the switch region is given by

$$V = 2\pi R_c l * dr \quad (3)$$

where  $R_c$  [m] is the radius of the cathode,  $l$  [m] is the length of the switch region and  $dr$  [m] is the depth of the surface layer. The value of  $dr$  is given by  $dr = 0.5 * m * 2.866 \times 10^{-10}$ , where  $m$  is the number of monolayers desorbed. The BCC lattice contains two atoms/cell, therefore the number of atoms desorbed is given by

$$n = \frac{2\pi R_c l m}{(2.866 \times 10^{-10})^2} \quad (4)$$

#### B. NEUTRAL DENSITY PROFILE

The radial expansion of the neutral carbon layer is determined by

$$r = \left[ t - \frac{(R_s - R_c)}{v_d} \right] * v_n \quad (5)$$

where  $R_g$  [m] is the off axis location of the plasma guns,  $t$  [s] is the delay time from plasma gun firing to generator firing,  $v_d$  [m/s] is the plasma drift velocity and  $v_n$  [m/s] is the neutral expansion velocity. The neutral particle expansion distance will be considered constant for the duration of the switching action due to the short time frame involved and the relatively slow expansion velocity of the neutrals.

Sub-regions are formed by dividing Equation 5 by the number of sub-regions desired. Initially, each sub-region is assigned an equal number of particles based on the calculation of Equations 4 and 5. The profile can be adjusted so as to weight the number of neutrals in a given sub-region as will be explained in Appendix A. From this number profile, a neutral density profile for each sub-region will be calculated from

$$n_n = \frac{N_R}{\pi l (R_o^2 - R_i^2)} \quad (6)$$

where  $N_R$  [ $m^{-1}$ ] is the number of particles per sub-region and  $R_o$  [m] and  $R_i$  [m] are the outer and inner radii of the given sub-region. This neutral density profile is important for determining the mean-free-path of the electrons within each sub-region.

### C. ELECTRON FLUX

The number of electrons flowing through the layer of desorbed neutrals is determined from the electron current density flowing through the cathode surface. For a given total current,  $I$  [A], and a given ion current,

$$I_i = n_i e v_d A_c \quad (7)$$

where  $A_c$  [ $m^2$ ] is the cathode surface area, the electron flux at the anode is determined by

$$\Gamma = \left[ \frac{I - I_i}{e A_a} \right] * 10^{-9} \quad (8)$$

where  $A_a$  [ $m^2$ ] is the anode surface area and  $\Gamma$  has the units [number of electrons per square meter per nanosecond]. The electron current is extracted from the anode surface while the ion current is extracted at the cathode surface.

Conservation of charge requires that the electron current extracted at the anode must equal the electron current at the cathode. Therefore, the radially outward electron flux into a cylindrical region is given by

$$\Gamma_{in} = \Gamma \left[ \frac{R_a}{R_i} \right] \quad (9)$$

where  $R_i$  [m] is the radius of the inner surface that the electrons flow through. The number of incident electrons per nanosecond into each cylindrical region can be expressed by

$$N_e = \left[ \frac{I - I_i}{e} \right] * 10^{-9} \quad (10)$$

which is constant for a given current.

#### D. DENSITY OF IONIZED PARTICLES

The mean-free-path of the electrons is determined by

$$\lambda = (n_n \sigma)^{-1} \quad (11)$$

where  $\sigma$  [ $m^2$ ] is the electron impact ionization cross section for the given target material. The value of  $\sigma$  is dependent only on the energy of the incident electrons. Table 1 is used to determine the electron impact ionization cross section for neutral carbon atoms [Ref. 9]. The values used range from relatively low energies ~ 20 eV up to ~ 1000 eV. It is assumed that the ionization occurs at low voltages so only relatively low electron energies will be considered. The values of energy are given in electron volts and the cross section is given in square meters.

The ionization of the neutral particle cloud is dependent on the electron flux, mean-free-path and the thickness of the medium. For a given flux of electrons incident upon a medium

of thickness  $x$  and mean-free-path, the flux of electrons exiting the medium is reduced by the factor  $\exp(-x/\lambda)$ . The difference between the incident and exiting electrons represents the ionization that occurs in the material.

TABLE 1  
ELECTRON IMPACT IONIZATION CROSS SECTION

Energy	Cross section	Energy	Cross section
20	1.00E-20	200	1.50E-20
30	1.80E-20	300	1.20E-20
40	2.10E-20	400	9.00E-21
50	2.30E-20	500	8.00E-21
60	2.40E-20	600	7.00E-21
70	2.30E-20	700	6.50E-21
80	2.20E-20	800	6.00E-21
90	2.15E-20	900	5.50E-21
100	2.10E-20	1000	5.00E-21

The number of neutral carbon atoms that are ionized can be expressed by

$$N_i = N_e [ 1 - \exp(-x/\lambda) ] \quad (12)$$

It follows that the density of the desorbed carbon atoms that become ionized is given by

$$n_i = \frac{N_i}{\pi l (R_o^2 - R_i^2)} \quad (13)$$

At the end of each nanosecond time increment, the number of particles that become ionized in each region is subtracted from the original number. The new densities, mean-free-

paths, etc. are then recalculated for the next nanosecond increment.

#### E. DENSITY RATIO AND PRESSURE GRADIENT

The ratio of the ionized carbon particles to the plasma density is given by

$$D = \frac{n_t}{n} \quad (14)$$

where  $n_t$  [ $m^{-3}$ ] =  $n_i + n$ , is the total ionized density. The electric field at the cathode and the sheath width are influenced by increased values of  $D$ . The electric field experienced at the cathode can be modified by multiplying Equation 2 by  $D^{1/2}$  which demonstrates the influence of the ionization on the electric field.

In addition to the influence of  $D$  on the electric field experienced at the cathode, an increasing  $D$  produces a pressure force within the plasma. Treating the plasma as an ideal gas, the pressure can be expressed as  $p = nkT$ , where  $k$  [J/K] is the Boltzmann factor and  $T$  [K] is the electron temperature of the plasma. Considering only the pressure gradient force, the electric field produced by the gradient can be expressed by

$$E = - \frac{kT}{en_d} \nabla n \quad (15)$$

where  $n_d$  [ $m^{-3}$ ] is a modified density term. This term is the average density between adjacent regions and is given by

$$n_d = \frac{n_t + n}{2} \quad (16)$$

If the pressure gradient force is sufficiently strong, the motion of the ions and electrons in this region will be affected.

#### IV. RESULTS

The results of this study are presented in two parts. First, the ionization occurring in the desorbed carbon cloud is evaluated. Second, the effect of the pressure gradient on the electric field due to the ionization is considered. The switch parameters and the input current used in this study are taken from the Gamble I experiments reported in Reference 10. The effect of varying the switch parameters on the ionization and resultant electric field strength is also evaluated.

Typical switch parameters given in References 1, 2, 4 and 10 are shown in Table 2.

TABLE 2  
SWITCH PARAMETERS

Gun Plasma Density	$3.0 \times 10^{19} \text{ m}^{-3}$
Plasma Drift Velocity	$7.0 \times 10^4 \text{ m/s}$
Delay time	$1.5 \times 10^{-6} \text{ s}$
Time of flight	$1.36 \times 10^{-6} \text{ s}$
Cathode radius	$2.5 \times 10^{-2} \text{ m}$
Anode radius	$5.0 \times 10^{-2} \text{ m}$
Gun-cathode distance	$9.5 \times 10^{-2} \text{ m}$
Switch length	$4.0 \times 10^{-2} \text{ m}$

##### A. IONIZATION RATIO

The switch parameters listed in Table 2 which will be varied during the evaluation are the density of the plasma guns and the delay time between the firing of the plasma guns

and the firing of the generator. In addition, the effect of the electron energy, monolayers desorbed and the density profile of the desorbed particles will be considered.

#### 1. Density profile

The density profile utilized is explained in Appendix A. Essentially, the expanding carbon cloud is divided into 5 concentric annular regions of equal spacing. Each region is assigned an equal number of neutral carbon particles. This method produces a slightly non-uniform density profile due to the cylindrical geometry. However, the profile can be altered by applying a weighting factor  $f$ . For  $f = 1$ , the number of particles in each region is equal. For  $0.5 < f < 1$ , the number of particles is more heavily weighted to the outer regions while  $1 < f < 2$ , more particles are allocated within the inner regions.

The effect of this particle weighting can be seen in Figures 2, 3, 4 and 5. For 50 eV electrons, the ionization of the carbon particles saturates within 40-45 nanoseconds. Allocating more particles in the outer regions produces a less varied plasma density difference between regions than allocating them to the inner regions. By weighting the inner region, an order of magnitude plasma density difference can be achieved.

#### 2. Desorbed layers

As seen in Figure 6, variations in the number or fractional number of monolayers desorbed affects the

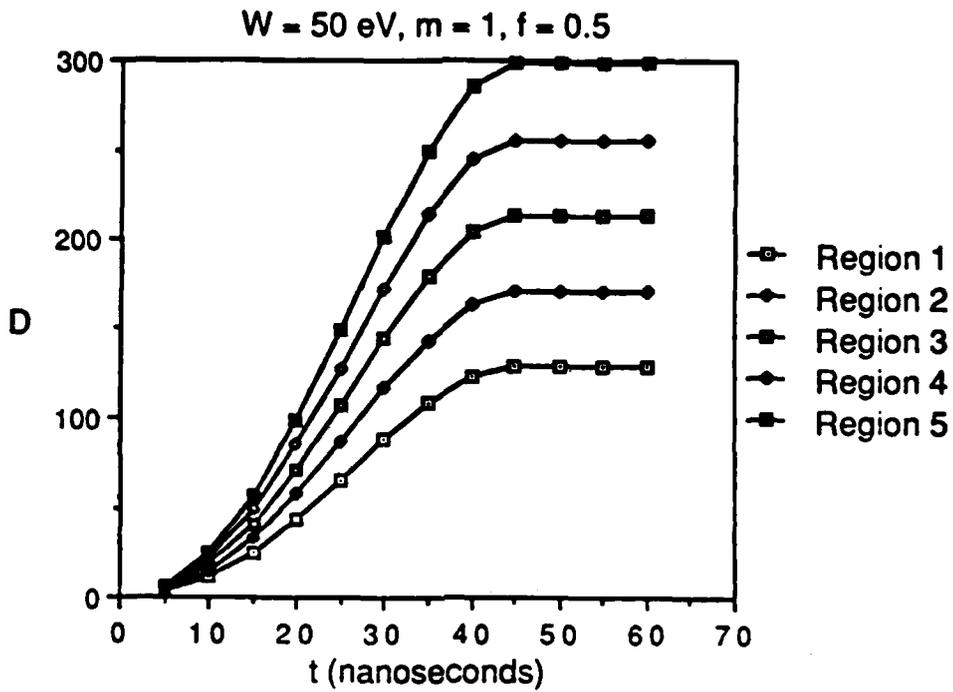


Figure 2. Density profile  $f=0.5$ .

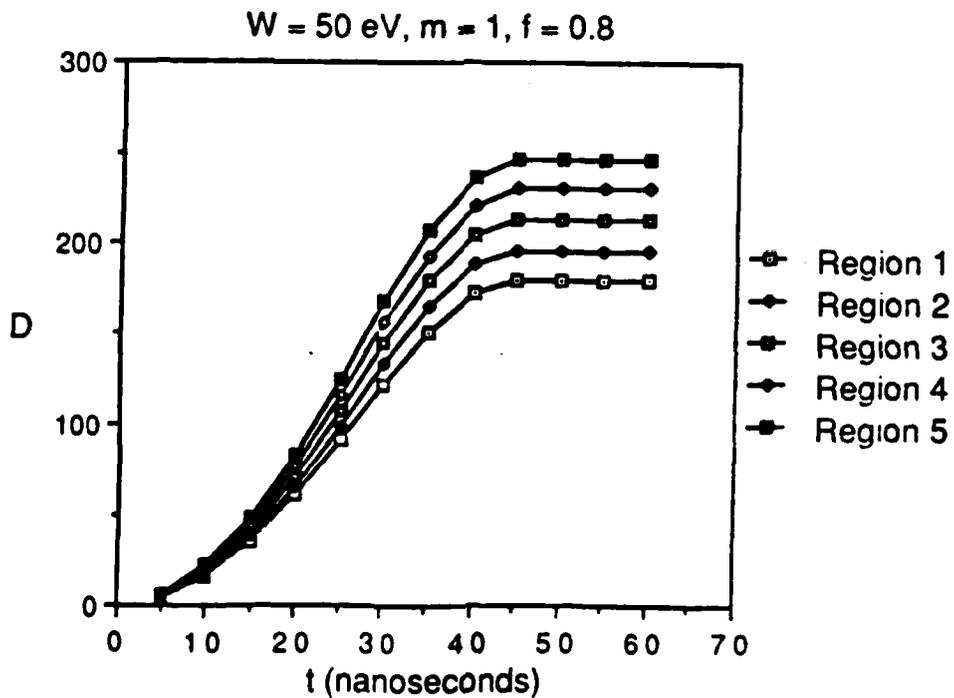


Figure 3. Density profile  $f=0.8$ .

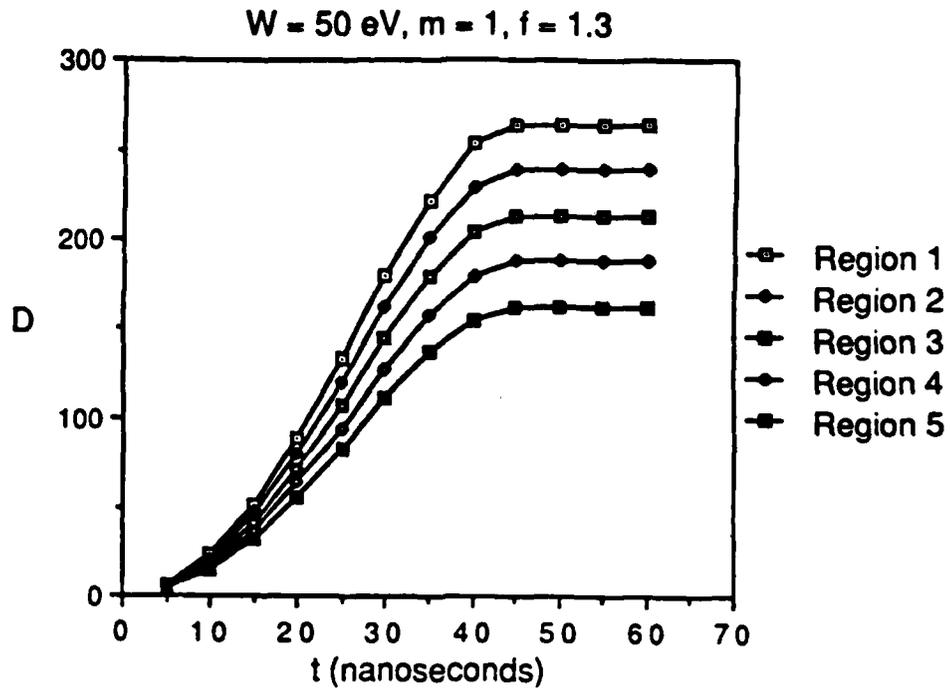


Figure 4. Density profile  $f=1.3$ .

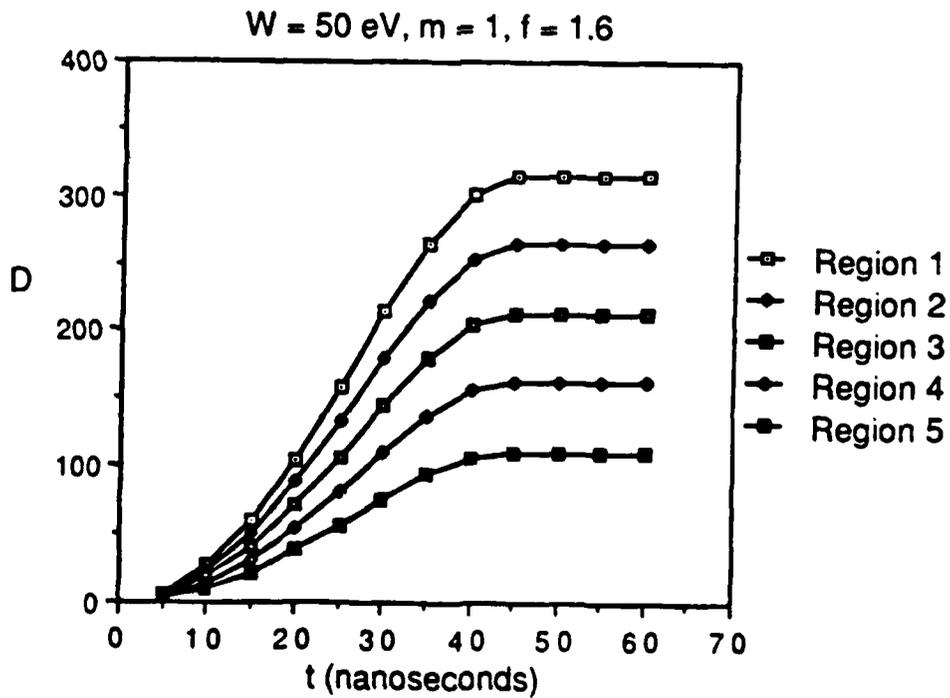


Figure 5. Density profile  $f=1.6$ .

ionization ratio by the same factor. Increase the number of monolayers desorbed by a factor of 10, and a factor of 10 increase in the ionization ratio is observed. This information provides a baseline to consider for the number of monolayers that must be removed in order to produce any significant effect on the electric field or the sheath width as proposed by Schwirzke. Equations 1 and 2 scale with the square root of the plasma density. Figure 6 clearly demonstrates that in order to influence the electric field, at least 0.1 monolayers of carbon particles must be desorbed from the surface. In order to see the trends more clearly, one monolayer will be utilized for all future comparisons.

### 3. Electron energy variations

From Table 1, it is clear that electrons with energies below 100 eV have larger ionization cross sections than those of higher energies. Figure 7 demonstrates that the lower energy electrons ionize the carbon layer much more rapidly than the higher energy electrons. Based on the known time scales of the plasma opening switch, it can also be inferred that the voltage across the sheath must remain relatively low ( $20 \leq f \leq 100$ ) during the initial conduction phase of the current. This allows for rapid plasma density increase near the cathode surface. However, the electric field in Equation 2 is dependent on the density and the applied voltage. If the anode-cathode potential difference remains low, then the density must increase significantly to

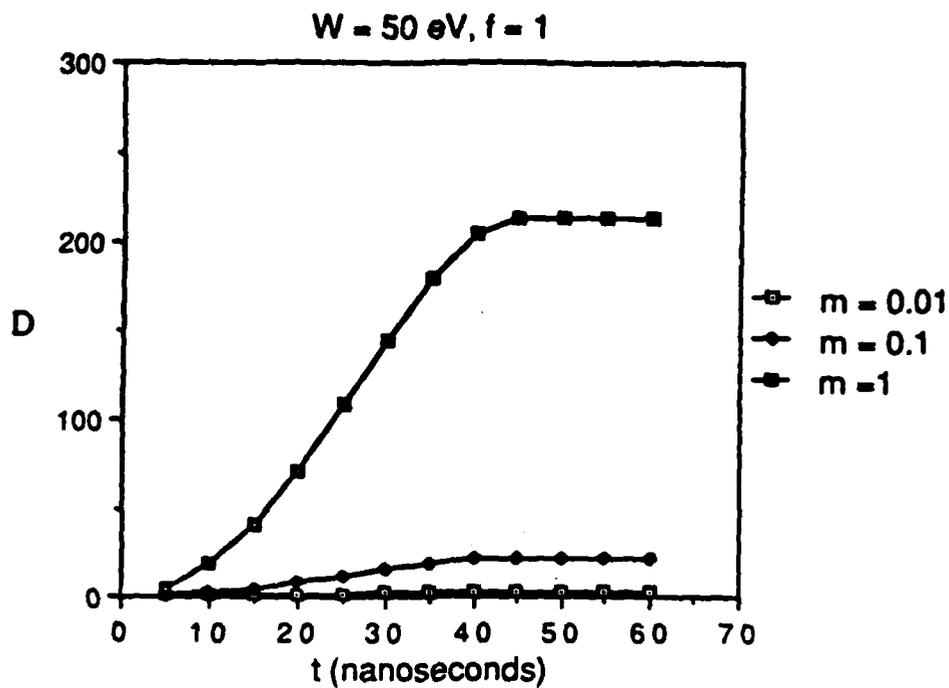


Figure 6. Desorption variation.

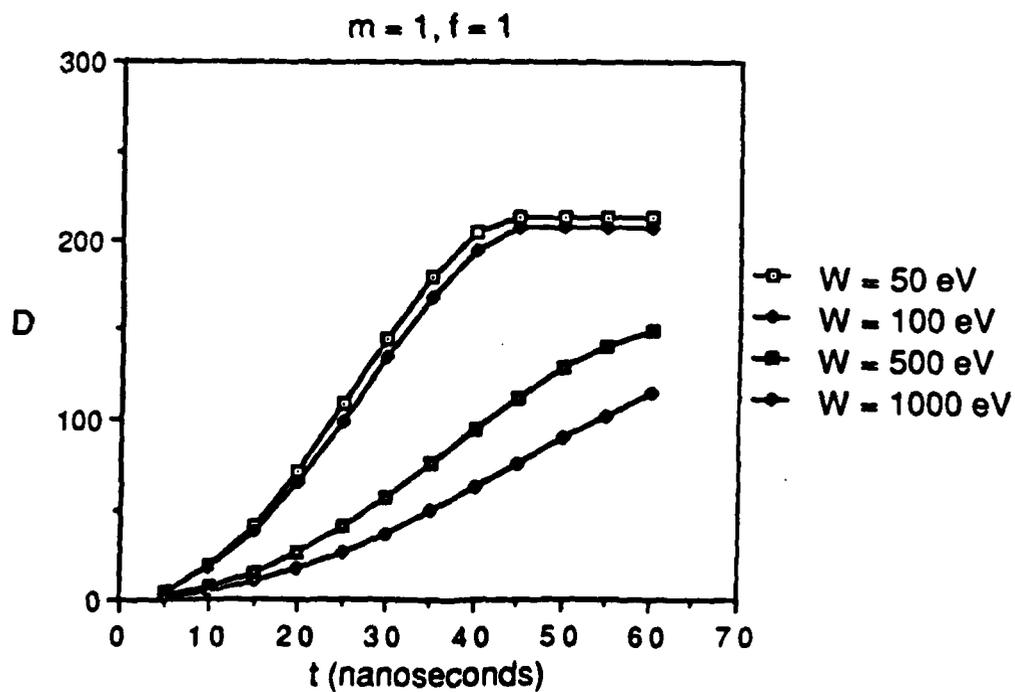


Figure 7. Energy variation.

provide the electric fields necessary to sustain electron emission.

#### 4. Delay time

By varying the delay time between the firing of the plasma guns and the generator, the size and density of the desorbed carbon cloud are modified. This results in an overall decrease in the ability of the electrons to ionize the carbon atoms as the delay time increases. As stated previously, the effect of the neutral carbon density on the mean free path is significant. Figure 8 demonstrates this as the density ratio  $D$  decreases as the delay time increases.

#### 5. Plasma gun density

As the plasma gun density varies, the ionization ratio also varies. Increased plasma gun densities require that the ionization of the carbon atoms be much greater before the effect is noticeable. Whereas decreased plasma gun densities can produce a significant ionization ratio almost immediately. Figure 9 demonstrates this principle.

### B. PLASMA DENSITY GRADIENT EFFECT

The plasma density gradient produces a pressure force in the vicinity of the cathode surface. The influence of the density gradient on the plasma particle motion is more difficult to assess with the given information. The data presented is static while the effect of the density gradient is dynamic in nature.

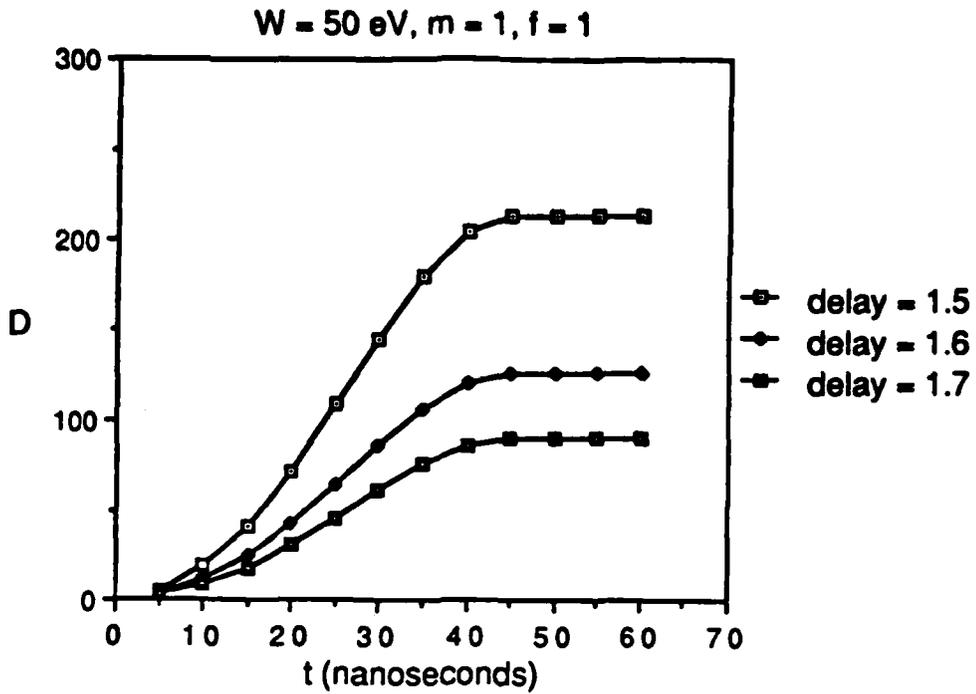


Figure 8. Delay time variation.

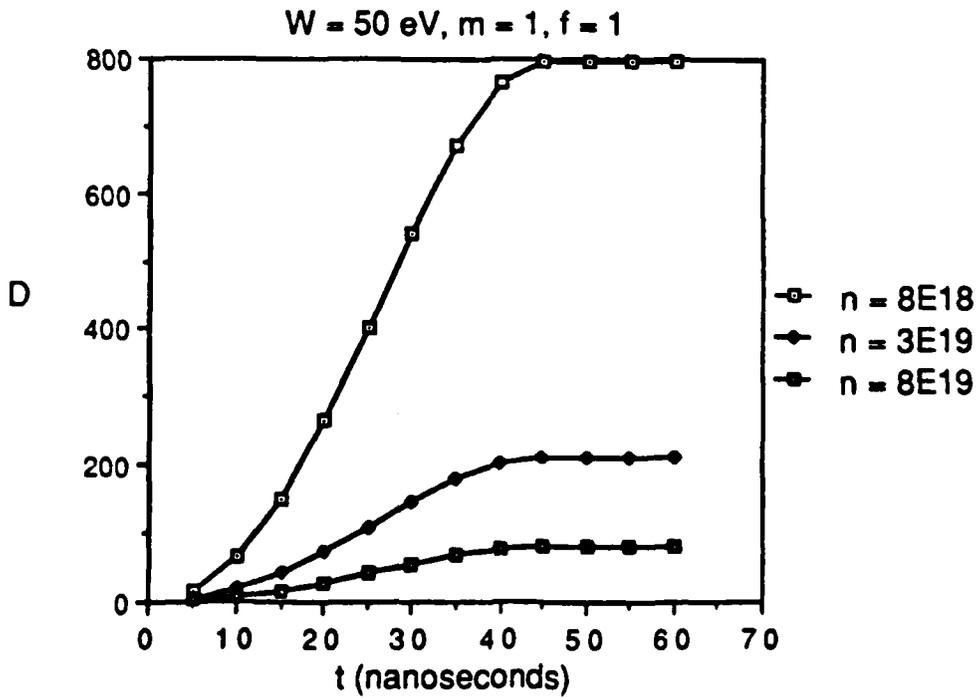


Figure 9. Gun density variation.

The carbon atoms forming the neutral cloud do not "feel" the effect of the electric field. Therefore, the ionization of the neutral particles is not affected by the density gradient. The ionized particles, on the other hand, will be accelerated by the electric field toward the cathode or anode depending on the charge and direction of the field at that point in space.

The electric field profile due to the density gradient will be of the form presented in Figure 10 where negative  $E$  represents the direction toward the cathode and positive  $E$  is toward the anode. The data for the electric field produced by the plasma density gradient is presented only between the cathode surface and the first annular region.

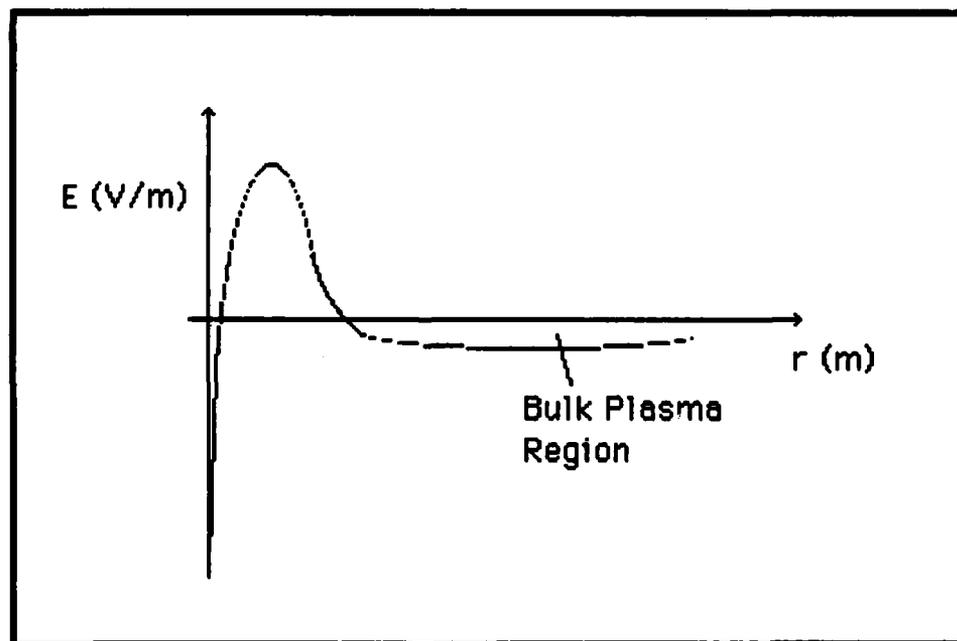


Figure 10. Electric field profile.

Figures 11, 12, 13, 14, and 15 show that the electric field due to the density gradient rapidly saturates. The reason for this is that Equation 15 becomes constant when the ratio D becomes large for a fixed electron energy. Equation 15 then becomes a function of the distance over which the gradient is calculated. This is essentially a function of the expansion time of the neutral carbon cloud as shown in Figure 14. In addition, the energy of the plasma also affect the electric field of Equation 15 as shown in Figure 13.

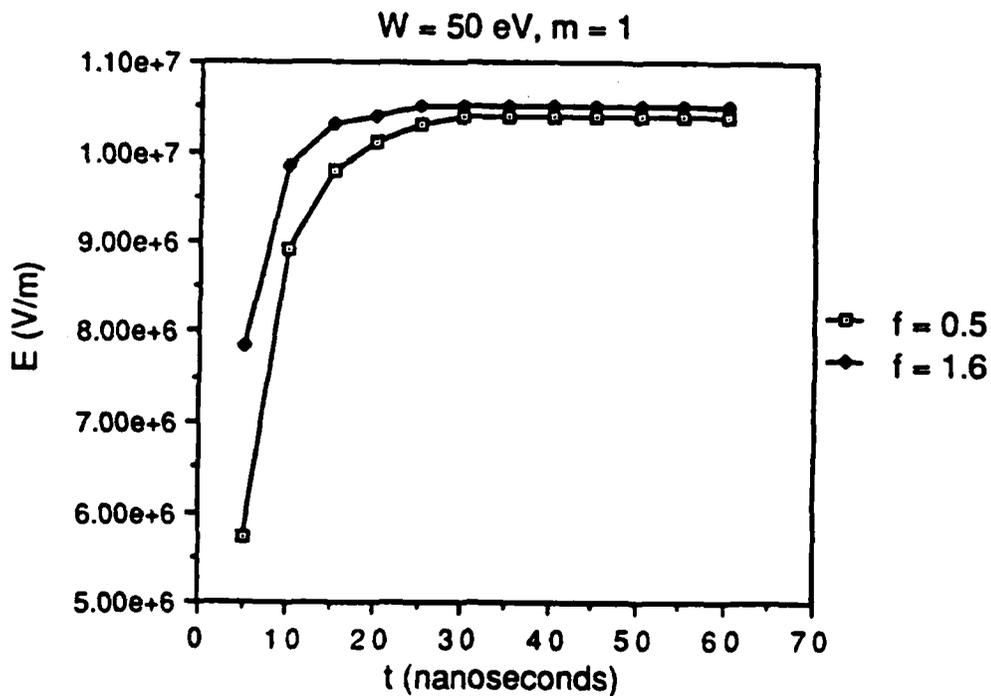


Figure 11. Density profile variation.

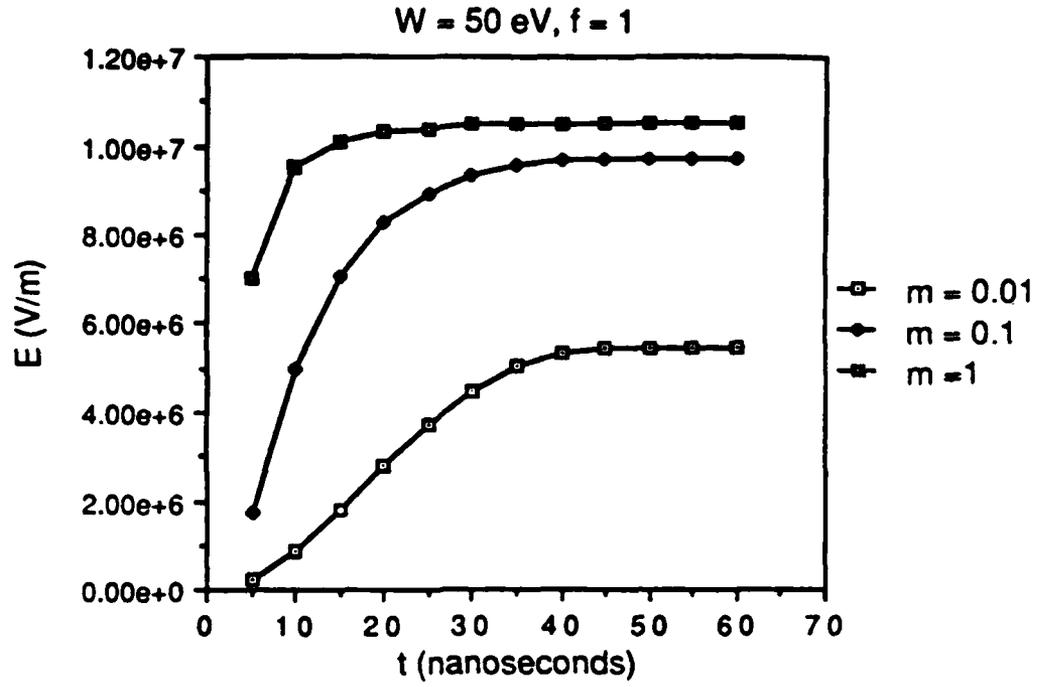


Figure 12. Desorption variation.

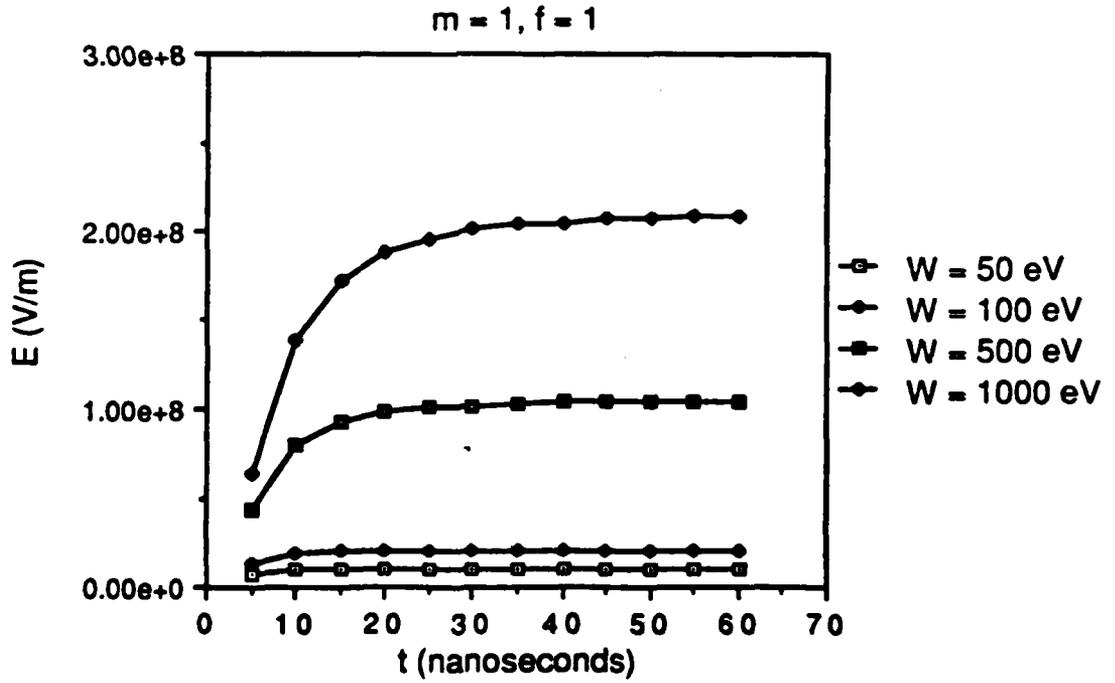


Figure 13. Energy variation.

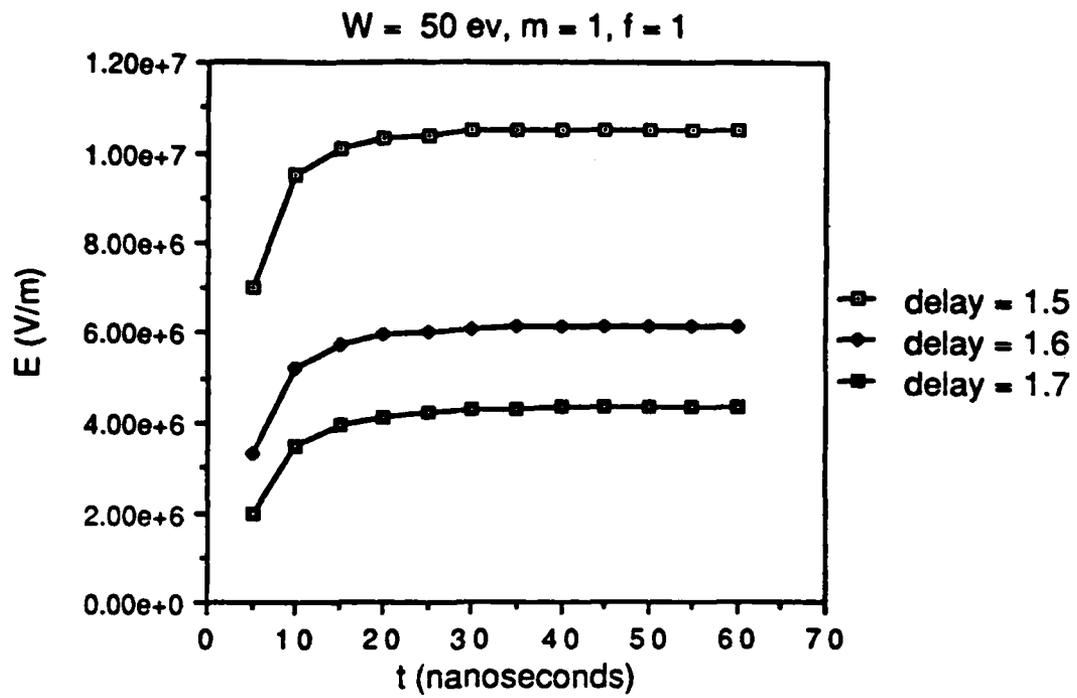


Figure 14. Delay time variation.

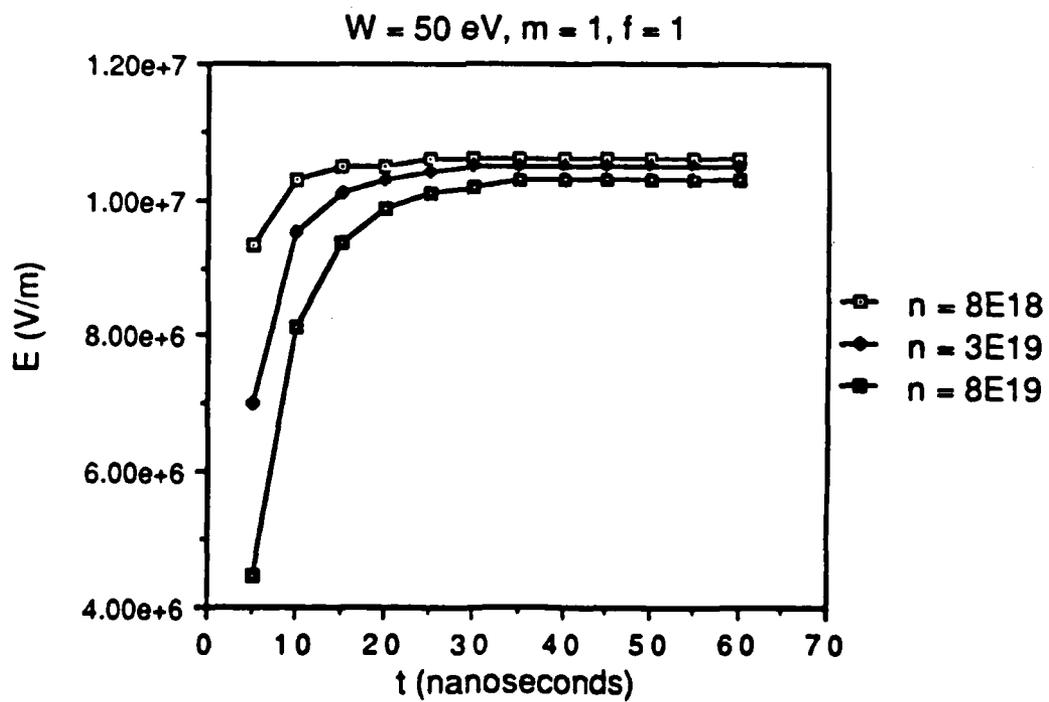


Figure 15. Gun density variation.

## V. CONCLUSIONS

The purpose of this study was to conduct some preliminary testing of Schwirzke's Plasma Sheath Model in an effort to determine the effect of the neutral carbon ionization process on the electric field experienced at the cathode. Inherent in that attempt was the determination that ionization was indeed occurring. In addition, the effect of the plasma density gradient was considered.

It was shown that even if modest levels of surface contaminants were desorbed, ionization was appreciable. As a result of this study, a baseline level of desorbed particles was established. Although the results are approximations based on ideal conditions, this information may be helpful for future investigations.

It was shown that variations in the delay time, plasma density and the desorption level provided the most dramatic effects on the density ratio  $D$ . This, in turn, affects the electric field and the electron field emission current drawn from the cathode surface.

The most interesting effect of the neutral particle ionization, is the effect due to the plasma density gradient which was shown to produce significant electric fields near the cathode. This effect could prove to be significant in future studies for two reasons. First, the plasma density

gradient produces electric fields on either side of the ionizing region which are diametrically opposed. Second, the expansion of the ions is confined on one side by the cathode and essentially free on the anode side.

The electric field produced by the density gradient near the cathode accelerates the ions toward the cathode while the electrons are essentially trapped within the opposing electric fields near the location of  $E = 0$ . As the ions are lost to the cathode surface, the electrons form a negative space charge layer which reduces the emission of electrons from the cathode. This could allow the current to be transferred to the load. At the same time, the anode side of the density gradient produces an electric field which opposes the electron motion toward the anode. Depending on the rate of expansion and ionization, this electric field could be responsible for the observed flow of ions near the anode. As the dense plasma cloud continues to expand, the electric field is reduced and the density ratio approaches unity again.

The effects of the anode pressure gradient and rate of expansion were not included in this study. However, the dynamic effects of the density gradient and resultant electric fields could prove important.

LIST OF REFERENCES

1. Meger, R. A., Commisso, R. J., Cooperstein, G. and Goldstein, Shyke A., "Vacuum Inductive Store/Pulse Compression Experiments on a High Power Accelerator Using Plasma Opening Switches", Applied Physics Letters, v. 42, pp 943-945, 1 June 1983.
2. JAYCOR Report J206-85-002/6243, "Investigations of Plasma Erosion Switches and PRS Analytical Development", by P. F. Ottinger, R. E. Terry, J. M. Grossmann, B. V. Weber, 4 March 1985.
3. Bluhm, H., Bohnel, K., Genuario, R., Hoppe, P., Karow, H. U., Ratajczak, W., Rusch, D. and Schwirzke, F., "Plasma Opening Switch Experiments at the Pulsed Power Generators Pollux and Kalif", Proc. of the 6th Int. Conf. on High Power Particle Beams, Kobe, Japan, pp.855-858, June 1986.
4. Ottinger, P. F., Goldstein, S. A. and Meger, R. A., "Theoretical modeling of the plasma erosion opening switch for inductive storage applications", Journal of Applied Physics, v. 56, pp 774-784, 1 August 1984.
5. Meeting Record DNA Pulsed Power Review and SDIO Update, 13-15 May 1986, Las Vegas, Nevada, compiled and edited by E. E. Stobbs, R. J. Commisso and J. M. Neri, December 1986, Naval Research Laboratory, Washington, D. C. pp. 297-324.
6. Schwirzke, F., Brinkschulte, H., and Hashmi, M., "Laser-induced desorption of gas from metallic surfaces", Journal of Applied Physics, v. 46, pp 4891-4894, 1975.
7. Halbritter, J., "Dynamical Enhanced Electron Emission and Discharges at Contaminated Surfaces", Applied Physics A, v. 39, pp 49-57, January 1986.
8. Askeland, Donald R., The Science and Engineering of Materials, p 746, PWS Publishers, 1984.
9. Brook, E., Harrison, M.F.A., Smith, A.C.H., "Measurements of the Electron Impact Ionization Cross Sections of He, C, O, and N atoms", Journal of Physics B, v. 11, p 3115, 1978.

10. Weber, B. V., Comisso, R. J., Meger, R. A., Neri, J. M., Oliphant, W. F. and Ottinger, P. F., "Current distribution in a plasma erosion opening switch", Applied Physics Letters, v. 45, pp. 1043-1045, 15 November 1984.

## APPENDIX A NEUTRAL DENSITY PROFILE

The basic notion of the initial number and number density in each of the five concentric annular rings is presented in the body of Chapter II and Equations 5 and 6. The weighting factor is based on a straight line curve approximation where the number of neutral particles remains constant.

The inner most region is multiplied by the weighting factor  $f$ , which ranges as  $0.5 \leq f \leq 2$ . Figure A1 shows a schematic of the annular sub-regions around the cathode. The equation of the line then depends on the slope and the  $y$ -intercept. The  $y$ -intercept is determined by the factor  $f$  multiplied by the number of particles in the innermost region. The slope is determined by forcing the middle region to always have the same number of particles as was originally allocated.

This method of weighting is somewhat restrictive although for the purposes of this study, the factor  $f$  is easily identified. For example, for  $f = 1$ , each region has the same number of particles while  $f = 2$ , immediately alerts the observer that the inner region is heavily weighted with particles.

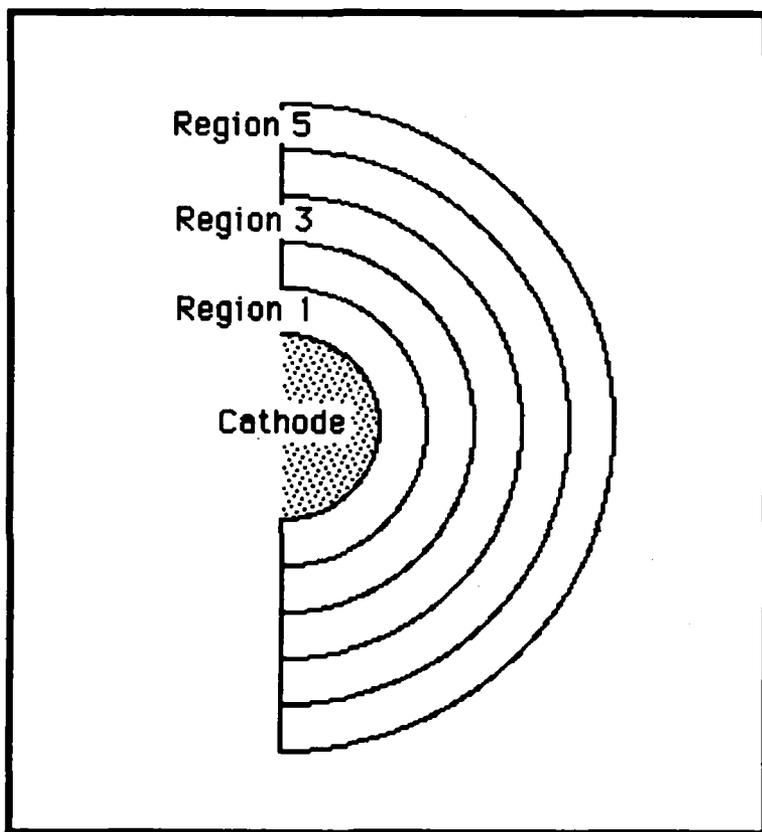


Figure A1. Annular sub-regions.

APPENDIX B PROGRAM LISTING

```
program sheath(input,output);
```

```
{The purpose of this program is to calculate the ionization  
of neutral particles which are desorbed from a cathode  
surface in a plasma opening switch configuration.  It also  
calculates the electric field produced by the density  
gradient.  Calculations used are based on fundamental plasma  
physics equations where no attempt has been made to apply  
kinetic theory.}
```

```
uses SANE;
```

```
const
```

```
charge = 1.6E-19;  
emass = 9.1E-31;  
imass = 2.004E-26;  
permi = 8.85E-12;  
cathradius = 2.5E-2;  
anoderadius = 5E-2;  
driftvel = 7E4;  
tvel = 330;  
swwidth = 4E-2;  
swlength = 9.5E-2;  
delay = 1.5E-6;  
iondensity = 8E19;
```

```
var
```

```
voltage, ivelocity, evelocity, current, selvolt, neutdensity,  
lamda, sigma, ncur, endcur, catharea, anodearea, eondensity,  
ji, je, x, ratio, neutradius,  
stepcur, irad, n, length, eflux, neutpart,  
partsinregion, f, left, slope, parts, lam, ionized:real;  
idens, deltat, dist, ri, ro, pos:extended;  
t, i, steps, k, j, m:integer;  
file1:text;  
ch:char;  
nparticles, iparticles, ndensity,  
idensity, ep:array [1..6] of real;  
match:boolean;
```

```
procedure setcon; {set the initial constants for the given  
parameters}
```

```
begin
```

```
iveLOCITY:=sqrt(2*charge*voltage/imass);
```

```

    evelocity:=sqrt(2*charge*voltage/emass);
    neutradius:=cathradius+(delay-swlength/driftvel)*tvel;
    x:=neutradius-cathradius;
    dist:=x/5;
    catharea:=2*pi*cathradius*swwidth;
    anodearea:=2*pi*anoderadius*swwidth;
    neutpart:=catharea*n*1.217E19;
end;

procedure cathodedensity; {determine the current density and
electron flux}
begin
    ji:=iondensity*charge*driftvel;
    je:=(current-(ji*catharea))/(anodearea);
    eflux:=je/charge*1E-9;if eflux<=0 then eflux:=1;
        {part/square meter nanosecond}
end;

procedure getinfo; {assume a straight line current profile}
begin
    write('Enter the anode-cathode voltage ');
    readln(voltage);
    write('Enter the number of monolayers to remove ');
    readln(n);
    write('Enter the starting current in kiloamps ');
    readln(ncur);
    current:=ncur*1E3;
    write('Enter the ending current in kiloamps ');
    readln(endcur);
    endcur:=endcur*1E3;
    write('Enter the number of steps to take ');
    readln(steps);
    stepcur:=(endcur-current)/(float(steps));
end;

procedure setsigma; {assign the proper cross section}
var
    setvolt:integer;
begin
    setvolt:=Round(selvolt);
    match:=TRUE;
    case setvolt of
        20: sigma:=1E-20;
        30: sigma:=1.8E-20;
        40: sigma:=2.1E-20;
        50: sigma:=2.3E-20;
        60: sigma:=2.4E-20;
        70: sigma:=2.3E-20;
        80: sigma:=2.2E-20;
        90: sigma:=2.15E-20;
        100: sigma:=2.1E-20;
    end;
end;

```

```

        200: sigma:=1.5E-20;
        300: sigma:=1.2E-20;
        400: sigma:=9E-21;
        500: sigma:=8E-21;
        600: sigma:=7E-21;
        700: sigma:=6.5E-21;
        800: sigma:=6E-21;
        900: sigma:=5.5E-21;
        1000: sigma:=5E-21;
    otherwise
        match:=FALSE;
    end;
end;

procedure profile; {write the equation of the line}
begin
    if f<>1 then begin
        left:=f*partsinregion;
        slope:=2*(1-f)*partsinregion/x;
        end;
    if f=1 then begin
        left:=partsinregion;
        slope:=0;
        end;
end;

procedure openfiles;
begin
    rewrite(file1,'data set 1');
end;

begin
    openfiles;
    match:=FALSE;
    while not match do begin
        getinfo;
        selvolt:=voltage;
        setsigma;
        end;

    setcon;length:=dist;
    partsinregion:=neutpart/10;
    writeln('Enter the factor ');readln(f);if f<0 then halt;
    profile;pos:=dist;

    write(file1,'voltage = ',voltage:11);
    write(file1,'length = ',x:11);
    write(file1,'monolayer = ',n:11);
    writeln(file1,'factor = ',f:11);
end;

```

```

for k:=1 to 5 do begin {assign the particles to the regions}
  nparticles[k]:=slope*(pos-dist/2)+left;
  iparticles[k]:=0;
  pos:=pos+dist;
end;

for i:=1 to steps do begin
  cathodedensity;ri:=cathradius;ro:=cathradius+dist;

for j:=1 to 5 do begin
  ndensity[j]:=nparticles[j]/(pi*swwidth*(sqr(ro)-
sqr(ri)));
  lamda:=1/(ndensity[j]*sigma);
  ionized:=(current/charge-ji)*1E-9*(1-exp((-
length)/lamda));
  iparticles[j]:=iparticles[j]+ionized;
  idensity[j]:=iparticles[j]/(pi*swwidth*(sqr(ro)-
sqr(ri)));
  nparticles[j]:=nparticles[j]-iparticles[j];
  if nparticles[j]<=0 then nparticles[j]:=1;
  ri:=ro;ro:=ro+dist;
end;

  if i mod 5 = 0 then begin {print out every 5 nanoseconds}
    write(file1,i:5);write(file1,' ');
    write(file1,voltage:11);
    write(file1,current:11);
    for m:=1 to 5 do begin
      write(file1,(idensity[m]+iondensity)/iondensity:11);
      end;
    write(file1,chr(9));
    ep[1]:=abs((2*solvolt)/(2*iondensity+idensity[1])*
(idensity[1])/dist);
    write(file1,ep[1]:11);
    for m:=2 to 5 do begin
      ep[m]:=abs((2*solvolt)/(idensity[m1]+idensity[m]+
(2*iondensity))*(idensity[m]-idensity[m-1])/dist);
      write(file1,ep[m]:11);
    end;

ep[6]:=abs((2*solvolt)/(idensity[5]+2*iondensity)*idensity[5]
/dist);
  writeln(file1,ep[6]:11);
  end;

current:=current+stepcur;
end;
close(file1);
readln;
end.

```

INITIAL DISTRIBUTION LIST

	No. Copies
1. Defense Technical Information Center Cameron Station Alexandria, Virginia 22304-6145	2
2. Library, Code 0142 Naval Postgraduate School Monterey, California 93943-5100	2
3. CPT Wenzel G. Evans Jr., USA 123 Shirley Lane Ballwin, Missouri 63011	2
4. Prof. F. Schwirzke, Code 61Sw Department of Physics Naval Postgraduate School Monterey, California 93943-5100	2
5. Prof. F. Buskurk, Code 61Bs Department of Physics Naval Postgraduate School Monterey, California 93943-5100	1

END

DATE

FILM

DTIC

2-85